Bubble formation in supersaturated gelatin: A further investigation of gas cavitation nuclei

David E. Yount and Chick M. Yeung

Department of Physics and Astronomy, University of Hawaii, Honolulu, Hawaii 96822
(Received 13 August 1980; accepted for publication 9 December 1980)

Recently, a new cavitation model has been proposed in which bubble formation in aqueous media is initiated by spherical gas nuclei stabilized by surface-active membranes of varying gas permeability. The data which originally motivated this development were obtained mainly by subjecting shallow gelatin samples to rectangular pressure schedules consisting of a rapid compression, equilibration of the sample at some constant increased pressure, and a rapid decompression. Since the initial pressure was ordinarily less than or equal to the final pressure, the magnitude of the initial compression was ordinarily greater than or equal to the magnitude of the final decompression. An equivalent statement for this type of schedule is that the initial overpressure was generally greater than or equal to the final supersaturation. The purpose of the experiment reported here is to test the surfactant cavitation model in the unexplored domain for which the reverse is true, i.e., for which the maximum overpressure is less than the final supersaturation. This domain can be reached by using slow compressions or stepped compressions which permit a significant rise in the dissolved gas tension while the ambient pressure is still increasing.

PACS numbers: 43.35.Ei, 43.25.Yw

INTRODUCTION

With the development of the gelatin model by Strauss[1] and LeMessurier,[2] a new assault on the related problems of inhomogeneous bubble nucleation and exogeneous gas bubble disease was begun. Transparent gelatin, subjected to various pressure schedules, is especially well suited for such a study since it yields a definite number of bubbles N that are stationary and can be counted and measured. Ultrasonic cavitation experiments, on the other hand, normally detect only bubble formation thresholds.[3-5] That is, they determine acoustic cavitation pressures along the one-dimensional line $N \sim 1$, but they do not explore the two-dimensional region $N \gtrsim 1$, which is accessible in gelatin.

Previous experiments in this series[1,6-9] were carried out mainly with rectangular pressure schedules such as that shown in Fig. 1. The maximum overpressure or crushing pressure is

$$p_{\text{crush}} = (p_{\text{amb}} - \tau)_{\max}, \tag{1a}$$

$$= p_m - p_0, \tag{1b}$$

and the maximum supersaturation is

$$p_{ss} = (\tau - p_{\text{amb}})_{\max}, \tag{2a}$$

$$\simeq p_s - p_f, \tag{2b}$$

where p_{amb} is the ambient static pressure, τ is the dissolved gas tension, p_0 is the initial pressure, p_m is the maximum pressure, $p_s = p_m$ is the saturation pressure, and p_f is the final pressure. Since p_f is ordinarily greater than or equal to p_0, p_{ss} is ordinarily less than or equal to p_{crush}:

$$p_{ss} \leq p_{\text{crush}}. \tag{3a}$$

The purpose of the present investigation is to explore the new pressure region defined by

$$p_{ss} > p_{\text{crush}}. \tag{3b}$$

This region is analogous to that probed in experiments which measure the tensile strengths of liquids by subjecting test samples to negative static pressure.[10] Ultrasonic cavitation experiments[3-5] generally have equal compressions and rarefactions and may approximate the condition $p_{ss} = p_{\text{crush}}$.[11] The region described

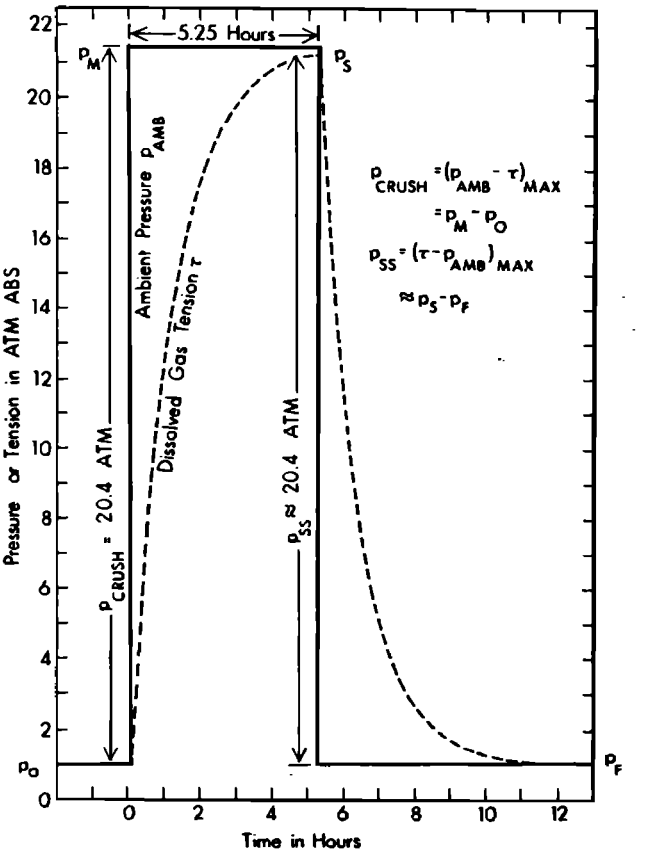

FIG. 1. Rectangular pressure schedule consisting of a rapid compression, equilibration of the sample at some increased pressure, and a rapid decompression. Since the final pressure p_f is ordinarily greater than or equal to the initial pressure p_0, the maximum supersaturation p_{ss} is ordinarily less than or equal to the maximum overpressure p_{crush}.

 0001-4966/81/030702-07$00.80

by Eq. (3b) can be reached *in vivo* by exposing subjects to high altitude or to isobaric counterdiffusion.[12,13] Finally, the new region can be studied by using slow compressions or stepped compressions which permit a significant rise in the dissolved gas tension τ while the ambient pressure p_{amb} is still increasing. For the schedule shown in Fig. 2, the maximum overpressure p_{crush} occurs on the first step and is simply the magnitude of the initial compression, 4.1 atm. The maximum supersaturation is $p_{ss} \simeq 20.4$ atm $\gg 4.1$ atm.

Our interest in the variables p_{ss} and p_{crush} is due in part to the experimental observation[8] that bubble counts in supersaturated gelatin depend only upon these pressure differences and not upon the absolute pressures *per se*. Furthermore, since p_{crush} is determined in a stepped compression by that increment which has the largest overpressure, any other increments, whether they precede or follow the largest, will have no effect. These generalizations are tested in the new pressure region along with a recently proposed cavitation model[11,14] outlined and extended in the Appendix.

I. MATERIALS, METHODS, AND RESULTS

The apparatus and procedures used in studying bubble formation in supersaturated gelatin are described elsewhere in detail.[8] We mention here only the salient features and those respects in which the present experiment differs from those reported previously.[1,6-9]

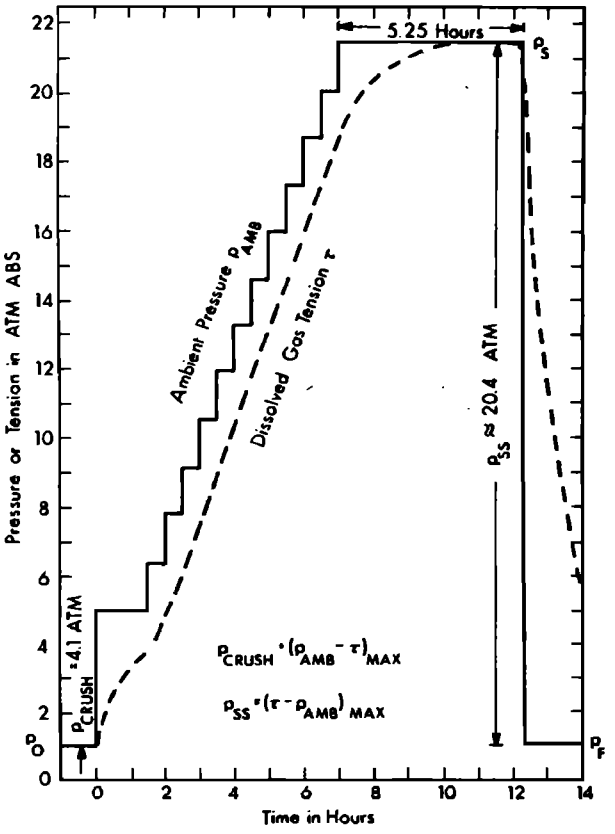

FIG. 2. Stepped compression schedule used to limit the overpressure p_{crush} without affecting the supersaturation p_{ss}.

For this series of runs, a new batch, gelatin batch E, was prepared and stored in individual 10-ml aliquots by freezing. Bubble counts from a given batch are ordinarily reproducible within statistical errors calculated from the square root of the number of bubbles, but significant differences have been noted between batches, even those mixed with the same stock of gelatin crystals.[1,8,9] Qualitatively, batch E is similar to batch A[1,6-8] and to batch D,[9] but there are some quantitative differences. Like batch D,[9] batch E was blended from high-yield and low-yield crystals. In this case, a low-yield mixture was selected because the region $p_{ss} > p_{crush}$ tends to be associated with small initial values of the critical radius for bubble formation, and some schedules of interest would otherwise produce bubbles too numerous to count.

Shortly before each run, the contents of one aliquot were thawed and pipetted into four separate glass counting chambers. The four samples, initially free of visible bubbles, were then subjected simultaneously to a particular pressure schedule causing macroscopic bubbles to form. The samples were 4 mm deep, and bubbles were counted in the lower 3 mm. This results in a fiducial volume of about 0.4 ml per sample. The experimental data thus consist of the bubble counts N and their respective pressure schedules. A small correction was made for the measured differences in fiducial volume among the counting chambers.[9]

The mean number of bubbles per sample is plotted in Fig. 3 for various combinations of p_{crush} and p_{ss} as defined, respectively, by Eqs. (1a) and (2a). The error bars indicate standard deviations from the mean and were calculated by combining in quadrature the square roots of the bubble counts for the individual samples. The dashed curves were drawn by eye through the data points for a particular value of p_{crush}. The solid curve representing $p_{ss} = p_{crush}$ was obtained by finding on each dashed curve that one point for which p_{ss} and p_{crush} are the same. Evidently, most of the data points lie in the new region $p_{ss} > p_{crush}$, and the isopleths for constant p_{crush} traverse the boundary $p_{ss} = p_{crush}$ without incident. The hypothesis[8] that the bubble counts N depend only upon p_{crush} and p_{ss} seems still to be viable, and our interpretation of p_{crush} as the maximum overpressure $(p_{amb} - \tau)_{max}$, rather than as the total compression $(p_m - p_0)$, appears also to be valid.

II. COMPARISON OF THE EXPERIMENT WITH THE SURFACTANT MODEL

In this section, we compare the experimental data in Fig. 3 with a particular type of surfactant cavitation model,[11,14] the so-called varying-permeability model, which is outlined and extended to nonzero skin thicknesses in the Appendix. We shall need only the model equations which describe nuclei whose surfactant skins are always permeable. In this special case, p_{ss} and p_{crush} are linearly related by the expression [Eq. (A1)][11,14]

$$p_{ss} = [2\gamma(\gamma_C - \gamma)/r_0^{min}\gamma_C] + [p_{crush}(\gamma/\gamma_C)], \quad (4)$$

where γ is the surface tension, γ_C is the crumbling

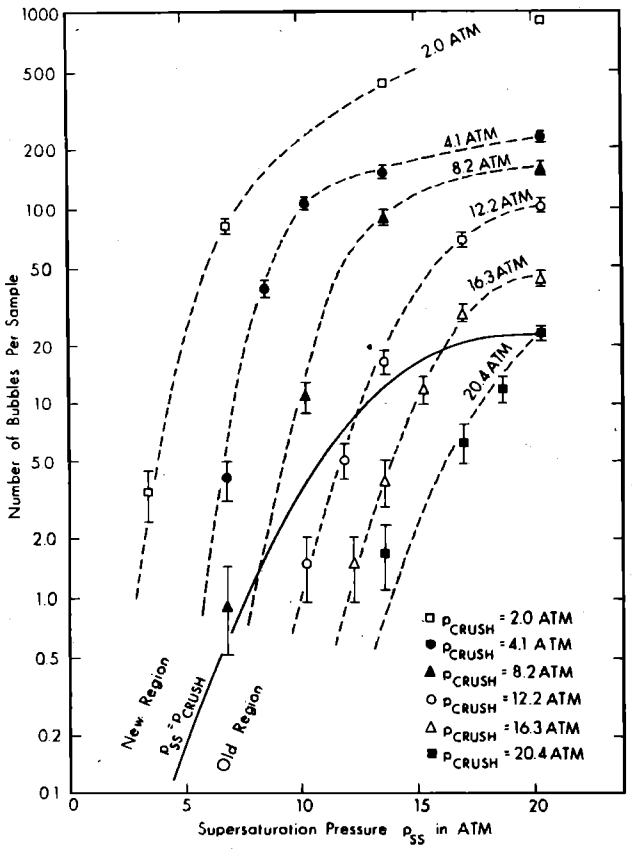

FIG. 3. Number of bubbles per 0.4-ml sample versus supersaturation pressure p_{ss} for six values of the maximum overpressure p_{crush}. Previous experiments were limited mainly to the old region $p_{ss} \leq p_{\text{crush}}$. Most of the present data points lie in the new region $p_{ss} > p_{\text{crush}}$.

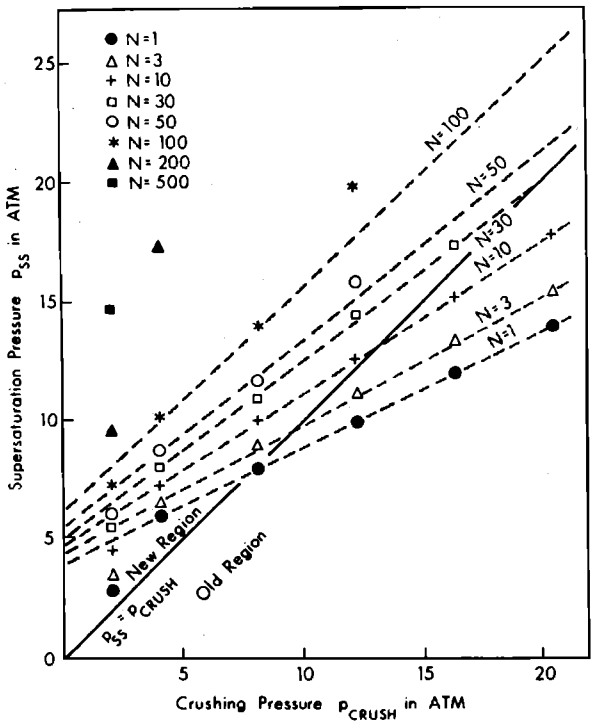

FIG. 4. Plot of p_{ss} versus p_{crush} for various numbers of bubbles N. In and near the old region the data points for the various bubble numbers seem to trace out straight lines that extend well into the new region.

compression of the skin, and $r_0^{\min}$ is the minimum value of the nuclear radius above which all nuclei originally in the sample will ultimately grow to form macroscopic bubbles.

In comparing the data with Eq. (4), we first obtain from Fig. 3 combinations of p_{ss} and p_{crush} which give fixed bubble numbers, such as $N = 1$, 3, 10, 30, 50, 100, 200, and 500. The results are replotted in Fig. 4 to yield p_{ss} versus p_{crush} for each of the values of N selected. As expected, all of the data points in the old region and many of those in the new can be described by a family of straight lines.

The second step in our analysis is to draw a set of straight lines through the appropriate points in Fig. 4. The values of γ_c/γ and $r_0^{\min}$ in Eq. (4) can now be determined for each straight line by following the procedure outlined in the Appendix. The resulting combinations of $(\gamma_c/\gamma, r_0^{\min})$ are plotted in Fig. 5 and can be described by another straight line

$$\gamma_c/\gamma = 1 + (7.5 r_0^{\min}/\mu\text{m}), \tag{5}$$

which is of the same form as Eq. (A4) derived from thermodynamic equilibrium considerations.[11] [The unit "μm" in Eq. (7) will cancel out when $r_0^{\min}$ is expressed in microns.]

For a measured surface tension of[8,9]

$$\gamma = (51 \pm 5)\,\text{dyn/cm}, \tag{6}$$

comparison of Eqs. (5) and (A4) gives

$$\beta_0 = 765\,\text{dyn/cm} - \mu\text{m}, \tag{7}$$

where β_0 is a measure primarily of the difference in chemical potential for surfactant molecules in the nuclear skin and in the surrounding reservoir.[11] Our value for β_0 is much larger than the result of 143 dyn/cm $-$ μm for gelatin batch A,[11] and this may be related to our lower bubble yields. More specifically, it appears that the low-yield crystals may contain substances which alter the relevant chemical potentials and decrease the cavitation rates by increasing β_0.

The integral radial distribution $N(r_0 \geq r_0^{\min})$ derived from our analysis is plotted in Fig. 6. A satisfactory parameterization for bubble numbers in the range $1 \leq N \leq 50$ is obtained with an expression of the form[11]

$$N = N_0 \exp(-r_0^{\min}/b), \tag{8}$$

which gives

$$N(\text{batch E}) = 265 \exp(-r_0^{\min}/0.0237\,\mu\text{m}) \tag{9}$$

nuclei or bubbles per 0.4-ml sample. This may be compared with

$$N(\text{batch A}) = 1200 \exp(-r_0^{\min}/0.088\ \mu\text{m}) \tag{10}$$

nuclei or bubbles per 0.4-ml sample obtained with batch A[11] and with

$$N(\text{batch D}) = 380 \exp(-r_0^{\min}/0.120\ \mu\text{m}) \tag{11}$$

nuclei or bubbles per 0.4-ml sample obtained with batch D.[9]

As in previous experiments,[8,9,11] Fig. 6 exhibits a departure from a pure exponential at small initial radii r_0^{min}. This is not an intrinsic property of the primordial radial distribution but results instead from a breakdown of the surfactant cavitation model as originally formulated.[11] In particular, it has already been suggested that the breakdown occurs because the finite thickness of the nuclear membrane has not been taken into account.[11] This is corrected in the Appendix by introducing a new parameter, δ, which is interpreted as the active skin thickness, i.e., as the thickness of that portion of the skin which is capable of supporting a pressure gradient. The result from Eq. (A7) is

$$p_{ss} = (\gamma/\gamma_C)\{(2\gamma_C/r_m^{min}) - [2\gamma/(r_m^{min} + \delta)]\}, \quad (12)$$

where the minimum radius r_m^{min}, following the maximum overpressure p_{crush}, can be calculated from[11]

$$p_{crush} = 2(\gamma_C - \gamma)[(1/r_m^{min}) - (1/r_0^{min})]. \quad (13)$$

We apply Eq. (12) to the present data sample as follows. First, we assume that the initial radial distribution is that given by Eq. (9) and plotted in Fig. 6. Since data in the model breakdown region were not used in extracting Eq. (9), the empirical function N(batch E) is insensitive to a finite skin thickness δ. The same argument holds for γ_C in Eq. (5), which is plotted in Fig. 5. In other words, N(batch E) in Eq. (9) and γ_C in Eq. (5) are regarded as "primordial" functions that characterize the nuclei in batch E before samples are subjected to various pressure schedules, and any discrepancies revealed later are interpreted as artifacts of our experimental and analytical techniques.

We next choose a value of N that is less than or equal to $N_0 = 265$ and calculate the corresponding values of r_0^{min} from Eq. (9) and γ_C from Eqs. (5) and (6). We then select a value of p_{crush} and calculate r_m^{min} from Eq. (13). The uncorrected value of p_{ss} is obtained by setting δ equal to zero in Eq. (12), and a tentative corrected value is found by substituting a trial skin thickness δ into the same equation. The procedure is repeated for different N, p_{crush}, and δ, and an attempt is made to describe all of the data points with the same δ. The results for $\delta = 0$ and $\delta = 0.00025$ μm $= 2.5$ Å are indicated by the solid and dashed lines, respectively, in Fig. 7.

It is evident from Fig. 7 that a finite skin thickness has very little effect at modest values of p_{ss} and p_{crush}. It cannot, for example, explain the discrepancies at $p_{crush} = 2.0$ atm. However, in the model breakdown region (upper right in Fig. 7), the difference between the dashed and the solid curves becomes quite large, approaching 10 atm in p_{ss} for $p_{crush} = 4.1$ atm. This resolves the disagreement between theory and experiment in this region, and a satisfactory description of all of the data above $p_{crush} = 2.0$ atm is now provided by Eq. (12) with $\delta = 2.5$ Å. It is, in fact, quite remarkable that so much has been gained by the introduction of a single parameter and parameter value. Furthermore, the manner in which δ has been introduced is both plausible and elementary in the context of the varying-permeability model.

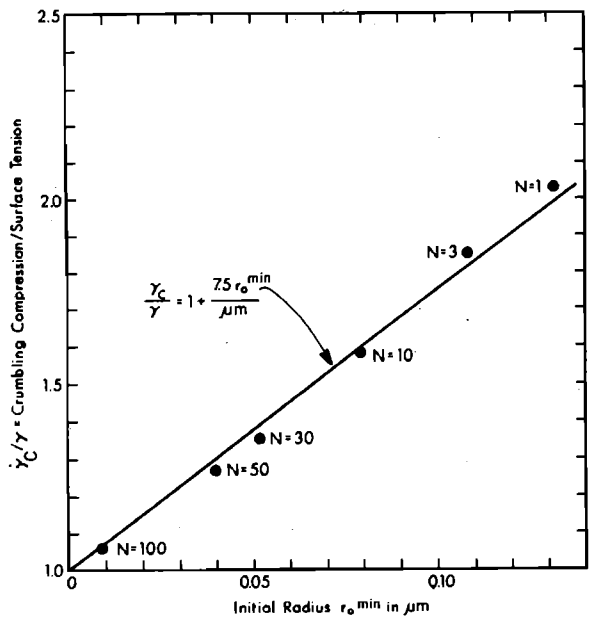

FIG. 5. Reciprocal of the slope $\partial p_{ss}/\partial p_{crush} = \gamma/\gamma_C$ versus the initial radius r_0^{min} for the dashed lines in Fig. 4. A linear dependence of γ_C/γ upon r_0^{min} is predicted in Ref. 11 from thermodynamic equilibrium considerations.

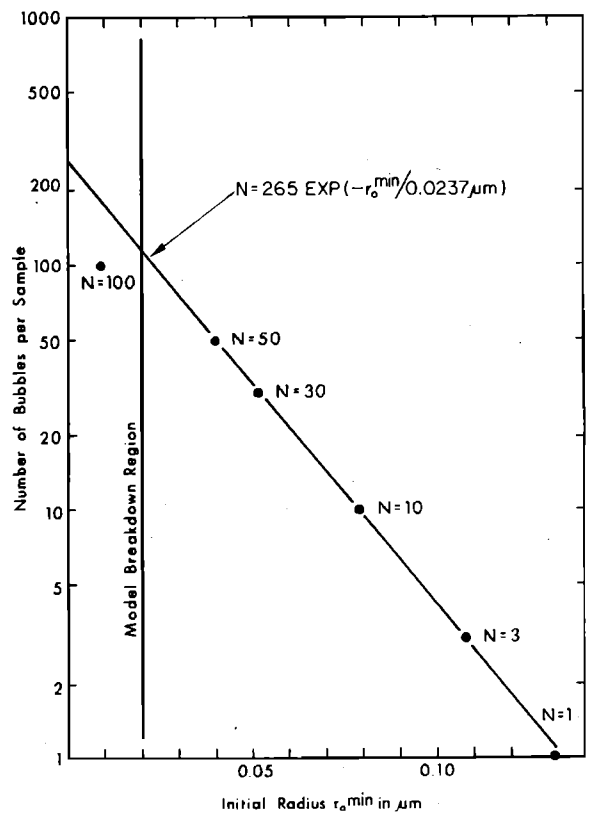

FIG. 6. Number of bubbles per sample versus minimum initial radius r_0^{min} for bubble formation. Within errors suggested by the scatter of the data points, the distribution is exponential outside the model breakdown region.

The quantity

$$S = 2kT/\beta_0 b \tag{14}$$

has been interpreted[11] as the area occupied by individual skin molecules, where k is the Boltzmann constant, T is the absolute temperature, and b is defined by Eq. (8). For $T = 294°K$, $\beta_0 = 765$ dyn/cm – μm, and $b = 0.0237$ μm, we obtain

$$S(\text{batch E}) = 45\ \text{Å}^2. \tag{15}$$

This is similar to the value of

$$S(\text{batch A}) = 65\ \text{Å}^2 \tag{16}$$

from batch A[11] and the value of

$$S(\text{batch D}) = 48\ \text{Å}^2 \tag{17}$$

from batch D.[9]

The magnitudes of the areas S are quite reasonable, and their consistency from batch to batch is impressive. Whereas it is easily conceivable that large changes could occur in β_0 or in b as a result of factors external to the nucleus itself, it would be difficult to explain a significant variation in the area occupied by an individual tightly-packed skin molecule. Conversely, if we assume that the area S per skin molecules is constant, then it follows from Eq. (14) that any change in β_0 would be matched by a reciprocal change in b. The decrease in cavitation rate associated with an increase in β_0 would then be due mainly, and perhaps entirely, to a steepening of the slope in the radial distribution $N(r_0 \geq r_0^{\min})$. This, in turn, would be accompanied by a general decrease in nuclear radii, including the model breakdown radius.

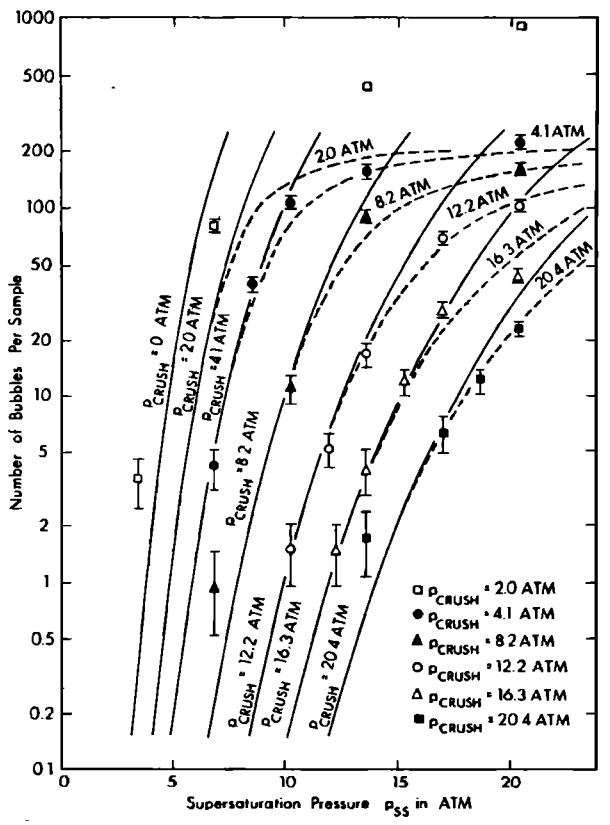

FIG. 7. Comparison of the original bubble counts with model calculations in which γ_C is found from Eqs. (5) and and (6), and the primordial radial distribution $N(r_0 \geq r_0^{\min})$ is given by Eq. (9). The solid curves, obtained from Eq. (4), correspond to a skin thickness of $\delta = 0$. The dashed curves, calculated from Eqs. (12) and (13), correspond to a skin thickness of $\delta = 2.5$ Å. This analysis resolves the model breakdown (upper right) seen in earlier experiments, but discrepancies remain in the new region for $p_{crush} = 2.0$ atm.

It has already been noted that the results at $p_{crush} = 2.0$ atm are aberrant. The salient features are as follows. First, the bubble counts are all much higher than the model extrapolations derived from the rest of the data points. Second, the bubble counts at $p_{ss} = 13.6$ atm and at $p_{ss} = 20.4$ atm (430 and about 900, respectively) are much higher even than $N_0 = 265$ bubbles or nuclei per 0.4-ml sample. Third, if we subtract from the observed bubble counts at $p_{crush} = 2.0$ atm the number expected from the above analysis, we obtain a "radial distribution" for the "surplus" nuclei that is not of the exponential form given in Eq. (8). These observations suggest that we may be dealing with a different type of nucleus to which the usual model equations do not apply. The "surplus" nuclei are easily crushed and must therefore be gasfilled and rather fragile. One class of objects that might fit this description is gasfilled crevices in suspended dust particles. Other types of surfactant nuclei could also be involved.

III. DISCUSSION

The distinctive feature of this experiment is the use of slow or stepped compressions which limit the overpressure p_{crush} without affecting the subsequent supersaturation p_{ss}. Pressure schedules of this type are of particular interest because they can be used to investigate cavitation nuclei of unusually small size. As in previous gelatin studies, most of the bubble counts reported here are in agreement with a naive surfactant model in which nuclei consist of spherical gas phases surrounded by a thin skin or membrane that is ordinarily gas permeable. Because of the smallness of the critical radii probed, however, many of our data points lie in the so-called "model breakdown region." This has permitted a systematic analysis of the breakdown phenomenon, including a demonstration that the surfactant model works well, even in the breakdown region, when the active skin thickness δ is taken into account. In other words, "breakdown" nuclei are also surfactant nuclei, and an elementary extension of the naive surfactant model suffices to describe them.

The experimental value of δ, about 2.5 Å, is too small to be the length of an aligned surfactant molecule *in situ*. On the other hand, 2.5 Å could plausibly represent the half-width of a spherical-shell potential well, whose minimum defines the effective nuclear radius. An outward displacement of 2.5 Å might then suffice to liberate a bound surfactant molecule by dislodging its polar head from the active layer. Similarly, since the polar heads would be pointing outward, it is plausible that the external surface pressure $2\gamma/r$ is transmitted through the surrounding reservoir or liquid

phase to within 2.5 Å of the effective radius, while the aligned hydrocarbon tails, pointing inward, passively convey the internal gas pressure to the same region. It should be evident from this discussion that a suitable basis for interpreting δ as the "active" skin thickness, rather than as the total membrane thickness, can be found either in a mechanical-pressure or a chemical-potential point of view. This duality is implicit in the equations which describe thermodynamic equilibrium of the surfactant molecules and which associate a pressure gradient with a gradient in chemical potential.[11]

Possible implications of the present investigation for the etiology and the prevention of exogeneous gas bubble disease are discussed in Refs. 12 and 13. Two earlier applications of the surfactant cavitation model to decompression sickness in rats and in humans are reported in Refs. 15 and 16.

ACKNOWLEDGMENTS

It is a pleasure to thank our colleagues Ed Beckman, Fred Kavanaugh, Tom Kunkle, and Jon Pegg for useful discussions and for constructive comments during the preparation of this manuscript. This work is a result of research sponsored in part by the University of Hawaii Sea Grant College Program under Institutional Grant Numbers 04-7-158-44129 and NA79AA-D-00085 from NOAA Office of Sea Grant, U.S. Department of Commerce.

APPENDIX: THE SURFACTANT MODEL

According to the surfactant model,[11,14] bubble formation in aqueous media is initiated mainly by spherical gas nuclei that are stabilized by elastic skins or membranes composed of surface-active molecules. An important goal of the model is to describe the way nuclear radii respond to changes in ambient pressure. For a given pressure schedule, one can calculate an initial minimum radius $r_0^{\min}$ above which all nuclei originally present in the sample will ultimately grow to form macroscopic bubbles.

It is implicit in the model calculations that nuclei *per se* are neither created nor extinguished by the pressure schedule and that the initial ordering according to size is preserved. That is, if nucleus "a" is smaller than nucleus "b" at the initial pressure p_0, then both nuclei are still present in the sample at the final pressure p_f, and nucleus "a" is still smaller than nucleus "b." This is referred to as the "ordering hypothesis." It follows that the number of bubbles N is uniquely associated with a radius $r_0^{\min}$ and that one can determine from a series of experiments the initial integral distribution $N(r_0 \geq r_0^{\min})$.

The "varying-permeability" model described in Refs. 11 and 14 is a type of surfactant model in which nuclear skins are initially permeable and become impermeable if p_{crush} exceeds some critical value $p^* - p_0$. All skins are permeable during decompression, and any changes in radius which might occur while the ambient pressure is held at the saturation pressure p_s are assumed to be negligible.

In comparing the data from this experiment with the varying-permeability model, only the ever-permeable equations corresponding to $p_{\text{crush}} \leq p^* - p_0$ are required. In this region, the model yields[11,14]

$$p_{ss} = [2\gamma(\gamma_C - \gamma)/r_0^{\min}\gamma_C] + [p_{\text{crush}}(\gamma/\gamma_C)], \tag{A1}$$

where γ is the surface tension, where $\gamma_C > 0$ is the "crumbling compression," i.e., the maximum value of the "skin compression" Γ, and where $r_0^{\min}$ is again the minimum value of the initial radius r_0 above which all nuclei in the sample will ultimately grow into macroscopic bubbles.

Application of Eq. (A1) to bubble counts in supersaturated gelatin[9,11] is based on the ordering hypothesis. The essential idea is that an isopleth of constant N is determined by the behavior of a single "critical" nucleus having fixed values of $r_0^{\min}$ and γ_C. Both parameters can have different values for different N, i.e., for a different critical nucleus. Eq. (A1) then yields a family of straight lines giving p_{ss} versus p_{crush} for constant N.

For each of the straight lines determined in the experiment, we can extract the slope

$$\partial p_{ss}/\partial p_{\text{crush}} = \gamma/\gamma_C, \tag{A2}$$

and the intercept $p_{ss}(p_{\text{crush}} = 0) = p_{ss}(0)$ to obtain the minimum radius

$$r_0^{\min} = 2\gamma[1 - (\gamma/\gamma_C)]/p_{ss}(0). \tag{A3}$$

The surface tension γ in gelatin has been directly measured.[8,9]

Another prediction of the varying-permeability model[11] is that the combinations of γ_C and $r_0^{\min}$ determined from the various isopleths of constant N should also be linearly related. The particular form,

$$\gamma_C/\gamma = 1 + (\beta_0 r_0^{\min}/2\gamma), \tag{A4}$$

has been derived from thermodynamic equilibrium considerations, where the constant β_0 is a measure primarily of the difference in chemical potential for surfactant molecules in the nuclear skin and in the surrounding reservoir.[11]

A breakdown of the varying-permeability model has already been reported.[8,9,11] This breakdown is associated with small values of the minimum radius $r_m^{\min}$ following the maximum overpressure p_{crush}, and it has been suggested that it results from the fact that the finite thickness of the nuclear membrane has not been taken into account.[11]

To remedy this situation, we take advantage of the fact that in the varying-permeability model all decompressions are permeable. The model equation for a permeable decompression from p_m to p_f is

$$-p_{ss} = 2(\gamma_C - \gamma)[(1/r_f^{\min}) - (1/r_m^{\min})], \tag{A5a}$$

where the final radius $r_f^{\min}$ can be found from the Laplace relation

$$p_{ss} = 2\gamma/r_f^{\min}. \tag{A5b}$$

Using Eq. (A5b) to eliminate $r_f^{\min}$ in Eq. (A5a), we obtain

$$p_{ss} = 2\gamma(\gamma_c - \gamma)/r_f^{\min}\gamma_c \quad \text{(A6a)}$$

$$= (\gamma/\gamma_c)[(2\gamma_c/r_m^{\min}) - (2\gamma/r_m^{\min})] \ , \quad \text{(A6b)}$$

which is valid in both the permeable and the impermeable region.

We now assume, after applying the overpressure p_{crush}, that the membrane is characterized by a radius $r_m^{\min}$ while the reservoir or surrounding liquid is characterized by a radius $r_m^{\min} + \delta$, where δ is interpreted as the "active" skin thickness, i.e., as the thickness of that portion of the skin which is capable of supporting a pressure gradient. Eq. (A6b) should then be corrected to give

$$p_{ss} = (\gamma/\gamma_c)\{(2\gamma_c/r_m^{\min}) - [2\gamma/(r_m^{\min} + \delta)]\}, \quad \text{(A7)}$$

where γ_c and $r_c^{\min}$ can be determined from data in the region where Eq. (A1) is valid and $r_m^{\min}$ can be calculated from Eq. (13). The active skin thickness is expected to be independent of p_{ss} and p_{crush}, and it can be evaluated by using Eq. (A7) to describe data in the region where Eqs. (A1) and (A6b) are breaking down.

[1]R. H. Strauss, Undersea Biomed. Res. 1, 169–179 (1974).

[2]D. H. LeMessurier, "Supersaturation and Preformed Nuclei in the Etiology of Decompression Sickness," paper presented at the Second International Meeting on Aerospace Medicine, Melbourne, 30 October–2 November, 1972 (unpublished).

[3]M. Strasberg, J. Acoust. Soc. Am. **31**, 163–176 (1959).

[4]M. Greenspan and C. E. Tschiegg, J. Res. Nat. Bur. Stand. 71C, 299–312 (1967).

[5]M. G. Sirotyuk, Akust. Zh. **16**, 237–240 (1970), Sov. Phys.–Acoust. **16**, 286–290 (1970).

[6]R. H. Strauss and T. D. Kunkle, Science **186**, 443–444 (1974).

[7]T. D. Kunkle and D. E. Yount, in *Sixth Symposium on Underwater Physiology*, edited by M. B. Kent (FASEB, Bethesda, 1975), pp. 459–467.

[8]D. E. Yount and R. H. Strauss, J. Appl. Phys. **47**, 5081–5088 (1976).

[9]D. E. Yount, C. M. Yeung, and F. W. Ingle, J. Acoust. Soc. Am. **65**, 1440–1450 (1979).

[10]R. E. Apfel, Sci. Am. **227**, 58–71 (1972).

[11]D. E. Yount, J. Acoust. Soc. Am. 65, 1429–1439 (1979).

[12]D. E. Yount, "Multiple Inert-Gas Bubble Disease: A Review of the Theory," paper presented at the Workshop on Isobaric Countercurrent Diffusion Phenomenon, Philadelphia, 13–14 November, 1979 (to be published).

[13]D. E. Yount, C. M. Yeung, and T. D. Kunkle, "Some Recent Experiments on Bubble Formation in Supersaturated Gelatin," paper presented at the Seventh Symposium on Underwater Physiology, Athens, 5–10 July, 1980 (to be published).

[14]D. E. Yount, T. D. Kunkle, J. S. D'Arrigo, F. W. Ingle, C. M. Yeung, and E. L. Beckman, Aviat. Space Environ. Med. **48**, 185–191 (1977).

[15]D. E. Yount, Aviat. Space Environ. Med. **50**, 44–50 (1979).

[16]D. E. Yount and D. A. Lally, Aviat. Space Environ. Med. **51**, 544–550 (1980).